

Sign change of tunnel magnetoresistance ratio with temperature in epitaxial Fe/MgO/Co₂MnSn magnetic tunnel junctions

M. A. Tanaka, T. Hori, K. Mibu, K. Kondou, T. Ono et al.

Citation: *J. Appl. Phys.* **110**, 073905 (2011); doi: 10.1063/1.3642963

View online: <http://dx.doi.org/10.1063/1.3642963>

View Table of Contents: <http://jap.aip.org/resource/1/JAPIAU/v110/i7>

Published by the [American Institute of Physics](#).

Related Articles

Angular-dependences of giant in-plane and interlayer magnetoresistances in Bi₂Te₃ bulk single crystals
Appl. Phys. Lett. **101**, 152107 (2012)

Magnetic field-dependent effective microwave properties of microwire-epoxy composites
Appl. Phys. Lett. **101**, 152905 (2012)

Giant magnetoresistance effect in graphene with asymmetrical magnetic superlattices
Appl. Phys. Lett. **101**, 152404 (2012)

Giant tunneling magnetoresistance in epitaxial Co₂MnSi/MgO/Co₂MnSi magnetic tunnel junctions by half-metallicity of Co₂MnSi and coherent tunneling
Appl. Phys. Lett. **101**, 132418 (2012)

Giant magneto-resistance estimated from direct observation of nanoscale ferromagnetic domain evolution in La_{0.325}Pr_{0.3}Ca_{0.375}MnO₃
J. Appl. Phys. **112**, 053924 (2012)

Additional information on J. Appl. Phys.

Journal Homepage: <http://jap.aip.org/>

Journal Information: http://jap.aip.org/about/about_the_journal

Top downloads: http://jap.aip.org/features/most_downloaded

Information for Authors: <http://jap.aip.org/authors>

ADVERTISEMENT



AIPAdvances

Now Indexed in Thomson Reuters Databases

Explore AIP's open access journal:

- Rapid publication
- Article-level metrics
- Post-publication rating and commenting

Sign change of tunnel magnetoresistance ratio with temperature in epitaxial Fe/MgO/Co₂MnSn magnetic tunnel junctions

M. A. Tanaka,^{1,a)} T. Hori,¹ K. Mibu,¹ K. Kondou,² T. Ono,² S. Kasai,³ T. Asaka,⁴ and J. Inoue⁵

¹*Department of Engineering Physics, Electronics and Mechanics, Nagoya Institute of Technology, Nagoya, Aichi 466-8555, Japan*

²*Institute for Chemical Research, Kyoto University, Uji, Kyoto 611-0011, Japan*

³*Magnetic Materials Center, National Institute for Materials Science, Tsukuba, Ibaraki 305-0047, Japan*

⁴*Department of Materials Science and Engineering, Nagoya Institute of Technology, Nagoya, Aichi 466-8555, Japan*

⁵*Department of Applied Physics, Nagoya University, Nagoya, Aichi 464-8603, Japan*

(Received 15 May 2011; accepted 15 August 2011; published online 5 October 2011)

Bias-voltage dependence of tunnel magnetoresistance (TMR) was investigated for epitaxial magnetic tunnel junctions of Fe/MgO/Co₂MnSn at various temperatures. The magnetoresistance measurement showed sign change of TMR ratio as a function of bias voltage. Sign change in TMR effect was also observed with changing temperature at a fixed bias voltage around 0 mV. These tunneling behaviors can be explained by a modified Jullière's model adopting an interaction between tunnel electrons and localized spins of magnetic impurities within the tunnel barrier. The temperature dependent sign change was qualitatively explained by the theoretical calculation. © 2011 American Institute of Physics. [doi:10.1063/1.3642963]

I. INTRODUCTION

The tunnel magnetoresistance (TMR) effect is a dramatic change of the resistance in magnetic tunnel junctions (MTJs) when magnetizations in two ferromagnetic layers change their alignment from antiparallel to parallel. Since the experimental findings of the TMR effect for MTJs with AlO_x barriers at room temperature,^{1,2} the TMR effect becomes one of key techniques for spin electronics devices, e.g., read heads in hard disk drives and magnetic random access memories. Further improvement of the TMR effect has been achieved by theoretical predictions of extremely high TMR ratios for Fe/MgO/Fe junctions,^{3,4} followed by experimental observations of high TMR ratios in epitaxial MTJs (Refs. 5 and 6). The observed values were slightly smaller than the predicted values, but the difference could be explained by suppression of the TMR value due to electron scattering at certain imperfections at the interfaces.⁷ At present, TMR ratio of more than 1000% has been observed in FeCoB/MgO/FeCoB junctions.⁸ Magnetic tunnel junctions with high TMR ratios having little influence from temperature and bias voltage are required for technological applications.

It is well known that TMR ratios decrease with increasing temperature. For example, the TMR ratio of FeCoB/MgO/FeCoB junctions decreases to around 500% at room temperature. The decrease has usually been attributed to electron scattering by magnon excitations.^{9,10} TMR ratios in MTJs with half-metallic electrodes show a tendency to decrease more rapidly with increasing temperature than those in MTJs with transition-metal electrodes. Magnetic tunnel

junctions with Mn-oxide electrodes show high TMR ratios at low temperature, but they decrease rapidly with increasing temperature, and become zero below Curie temperature.^{11–13} A possible mechanism of the strong temperature dependence is spin-flip tunneling caused by interactions between tunneling electrons and localized spins on Mn ions.^{14,15} Magnetic tunnel junctions with Heusler alloys also show rather strong temperature dependence in the TMR ratio,^{16–19} the mechanism of which has been attributed to local spin fluctuations, thermally unstable interfacial electronic states, etc.^{20–23} In general, the TMR ratios influenced by these mechanisms tend to approach zero with increasing temperature.

As for bias-voltage dependence of TMR ratios, all positive, all negative, and sign change types have been reported experimentally.^{17–19} An intrinsic mechanism for the sign change of the TMR effect as a function of bias voltage has been reported by Sharma *et al.*²⁴ They explained that the sign change is caused by the difference of the spin polarization of two barrier/electrode interfaces and by the sign change of the spin polarization with the bias voltage in one side. Several extrinsic mechanisms have been proposed for the bias-voltage dependence of the TMR sign; effects of interfacial electronic states,²² antisite Co atoms in Heusler electrodes,²³ oxidation of an Fe monolayer at the Fe/MgO interfaces,²⁵ effects of non-bonding states at interfaces,²⁶ and so on. In addition to MTJs with MgO tunnel barriers, an MTJ with a barrier made of an organic semiconductor Alq₃ also shows strong temperature and bias voltage dependence, which is accounted for donor-accepter-mediated transports in the tunnel barrier.²⁷ Thus, extrinsic mechanisms caused by a change in electronic states at or near the interfaces seem to affect the bias dependence of the TMR ratio strongly.

^{a)}Author to whom correspondence should be addressed. Electronic mail: mtanaka@nitech.ac.jp.

To obtain desirable temperature and bias voltage dependence of TMR ratios, it is important to clarify extrinsic factors which affect TMR effects. In this paper, we report that positive and negative TMR effects appear in Fe/MgO/Co₂MnSn MTJs as a function of bias voltage at room temperature and also as a function of temperature at a fixed bias voltage. Although the dependence of the TMR ratios on bias voltage could be attributed to extrinsic mechanisms mentioned above, the sign change of the TMR ratio with temperature, to our knowledge, has not been reported so far. Our results indicate that a certain extrinsic origin is responsible to the sign change in the TMR ratio with temperature. We explain the observed results adopting a modified Jullière's model, where interactions between tunneling electrons and localized spins within the insulator are introduced. We demonstrate how localized spins within the insulator can give rise to drastic temperature-dependent behaviors of the TMR ratio.

The paper is organized as follows. Sample preparation and measurement methods are explained in Sec. II, and observed results are presented in Sec. III. Discussion and model analysis for the sign change in the TMR ratio with temperature is given in Sec. IV, and the conclusion is given in the final section. The Appendix is devoted to the details of the model analysis.

II. EXPERIMENTALS

Layered structures of MgO (5 nm)/Cr (30 nm)/Fe (20 nm)/MgO (2.4 nm)/Co₂MnSn (26.1 nm)/Co (10 nm)/Cr (5 nm) were prepared on MgO (001) substrates using an electron beam deposition system. The bottom ferromagnetic Fe layer was deposited at room temperature and annealed at 350 °C in order to improve the crystallographic quality. After the deposition of the MgO barrier layer, the top ferromagnetic Co₂MnSn layer was prepared by depositing one atomic layer of Co, half an atomic layer of Mn and Sn alternately in a controlled manner at the substrate temperature of 400 °C. It is reported that Co₂MnSn layers grown at 400 °C have relatively uniform local magnetism.²⁸ The interface atoms of the Co₂MnSn layer on the MgO barrier were designed to be Mn and Sn. The Co layer was deposited on the layered structure to increase the coercivity of the upper Co₂MnSn layers. The crystal structures were characterized by reflection high-energy electron diffraction, x-ray diffraction, bright-field scanning transmission electron microscopy (bright-field STEM) and nano beam electron diffraction (NBED). Magnetic tunnel junctions were patterned into ellipse-shaped pillars of $6.0 \times 2.0 \mu\text{m}^2$ using a conventional photolithography and Ar ion milling process. Magnetoresistance measurements were carried out using a standard dc four-probe method. The positive current is defined as the current with the electrons flowing from the top Co₂MnSn layer to the bottom Fe layer.

III. RESULTS

Figure 1(a) shows a cross sectional bright-field STEM image of the layered structures. The image indicates that fully epitaxial Fe/MgO/Co₂MnSn MTJ structure with an

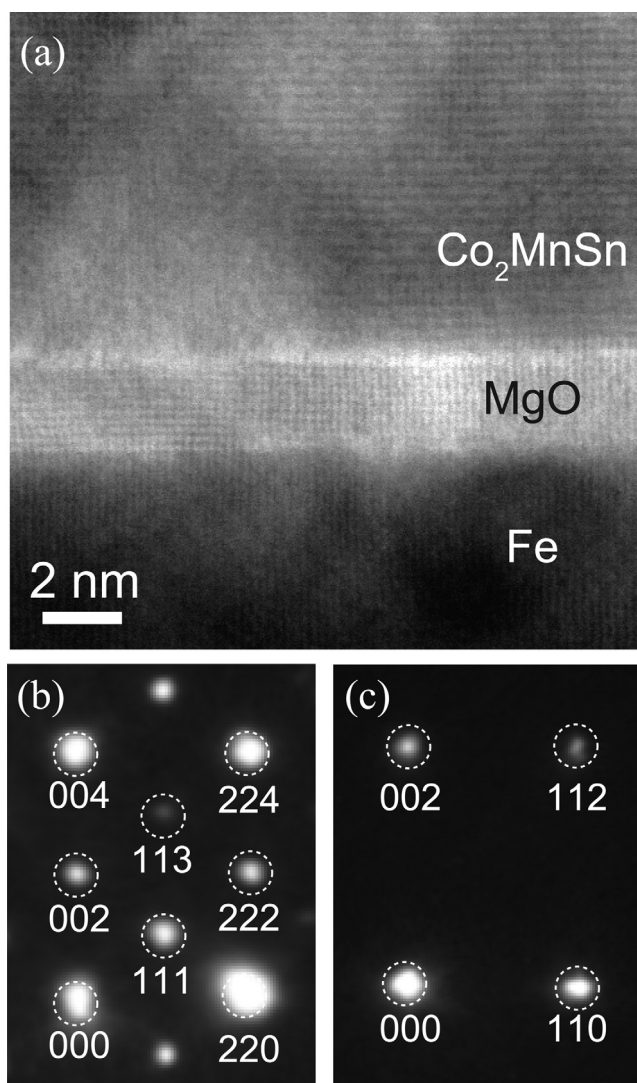


FIG. 1. (a) Cross sectional bright-field STEM image of the layered structures. (b) NBED pattern for the Co₂MnSn layer. (c) NBED pattern for the Fe layer.

atomically flat MgO barrier is realized. Figures 1(b) and (c) show NBED patterns for the Co₂MnSn and Fe layers, respectively. The patterns clarify that Co₂MnSn and Fe layers are grown epitaxially. The appearance of the Co₂MnSn (111) spot indicates that the Co₂MnSn layer has an L₂₁ structure. From the intensity ratio of Co₂MnSn (111) and (002) peaks of x-ray diffraction in polar plots, the degree of L₂₁ order of Co₂MnSn was estimated to be about 0.56 (Ref. 29).

Figure 2(a) shows magnetoresistance curves at various bias voltages at 300 K. Positive and negative TMR ratios of +5.9% and -10.3 % are observed at bias voltages of +500 mV and -200 mV, respectively. Figure 2(b) shows magnetoresistance curves at a bias voltage of +10 mV at 20 K, 150 K and 300 K. A negative TMR effect is observed at 300 K, whereas a positive TMR effect appears at 20 K.

Figure 3(a) shows bias-voltage dependence of TMR ratios for the epitaxial Fe/MgO/Co₂MnSn MTJ at various temperatures. The bias-voltage dependence of the TMR ratio at 300 K exhibits asymmetric characteristics with respect to the polarity, and negative TMR ratios are realized in the

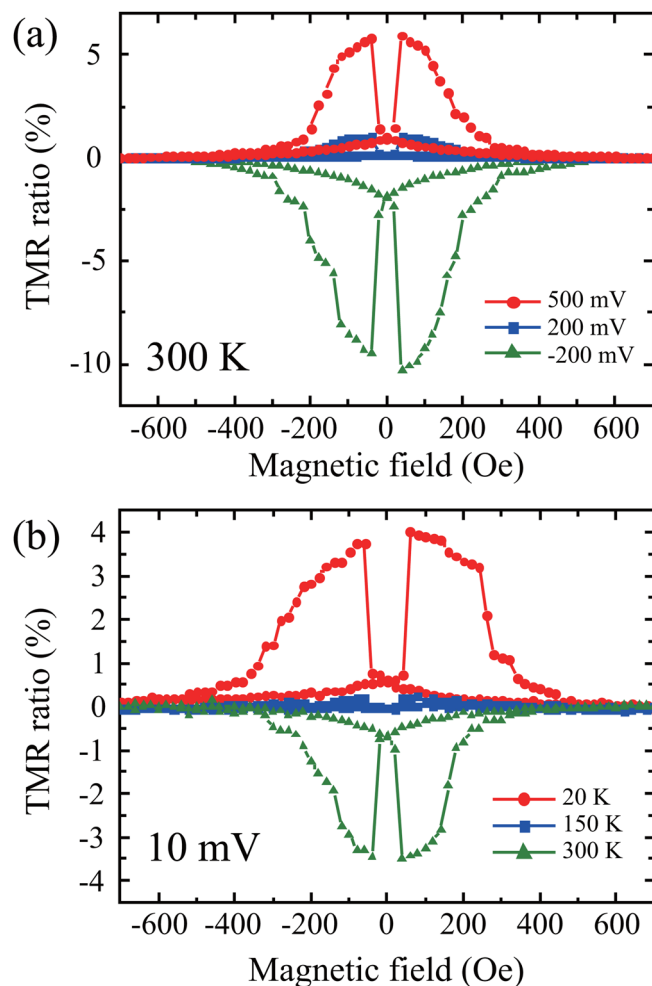


FIG. 2. (Color online) (a) Magnetoresistance curves for the epitaxial Fe/MgO/Co₂MnSn MTJ under various bias voltages at 300 K. (b) Magnetoresistance curves for the Fe/MgO/Co₂MnSn MTJ at a bias voltage of +10 mV at 20 K, 150 K and 300 K.

bias-voltage range between -600 mV and $+200$ mV, in contrast with typical TMR ratio which decreases monotonically as the magnitude of bias voltage increases. At low bias voltage, the TMR ratio changes from negative to positive with decreasing temperature. The sign change of the TMR effect with temperature is observed at bias voltage between -100 mV and $+150$ mV. Figure 3(b) shows bias-voltage dependence of resistance area (RA) products at antiparallel (AP) and parallel (P) magnetic configurations at 2 K and 300 K. The RA products for AP and P at 300 K exhibit large differences at -200 mV and $+400$ mV, which correspond to the minimum and maximum of the TMR ratio. As compared with the RA products in the AP configuration at 300 K, those at 2 K increase significantly at low bias voltage. This significant increase in RA products in the AP configuration at low bias voltage causes the sign change of the TMR effect with temperature.

Figure 4 shows temperature dependence of TMR ratios at bias voltages of -200 mV, $+10$ mV and $+400$ mV. At the bias voltages of -200 mV and $+400$ mV, no sign change of TMR ratio is observed with changing temperature. At the low bias voltage of $+10$ mV, the TMR ratio changes to positive with decreasing temperature. As shown in the next

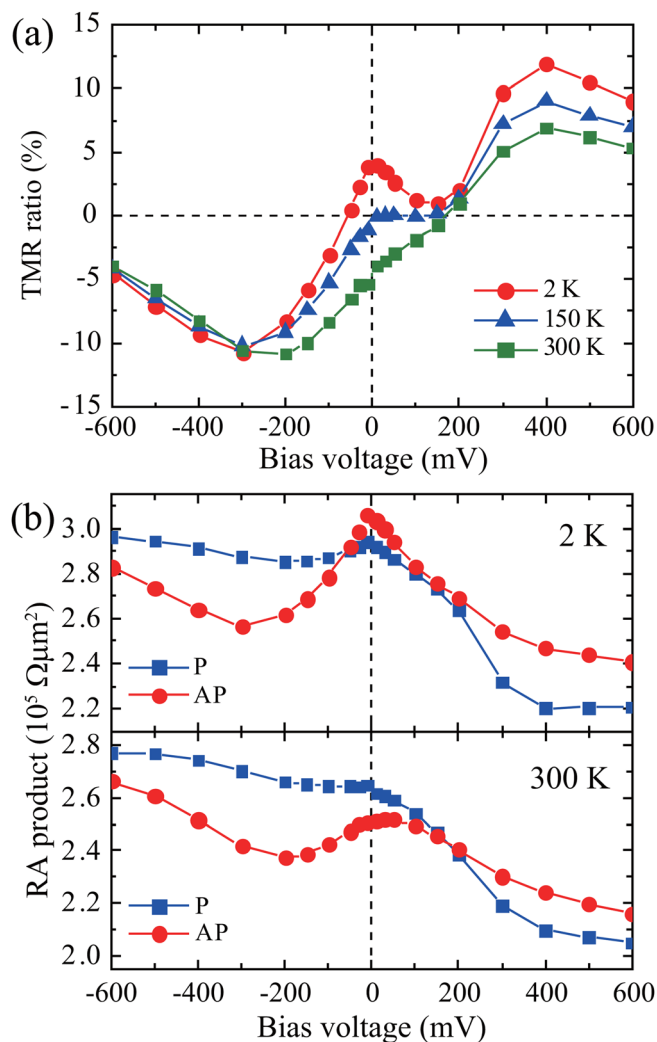


FIG. 3. (Color online) (a) Bias-voltage dependence of TMR ratios for the epitaxial Fe/MgO/Co₂MnSn MTJ at various temperatures. (b) Bias-voltage dependence of resistance area (RA) products at antiparallel (AP) and parallel (P) magnetic configurations at 2 K and 300 K.

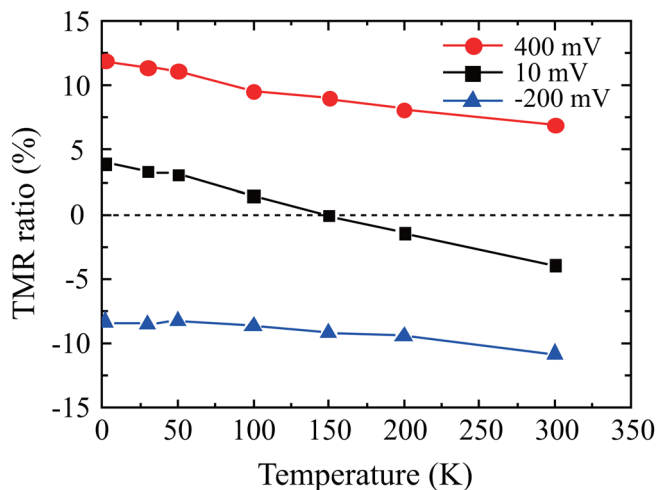


FIG. 4. (Color online) Temperature dependence of TMR ratios at bias voltages of -200 mV, $+10$ mV and $+400$ mV.

section, a modified Jullière's model can qualitatively explain the sign change of TMR ratio at bias voltage around 0 mV. We note here that the anomalous TMR behavior in the Fe/MgO/Co₂MnSn MTJs is more or less reproducible. For comparison with the Fe/MgO/Co₂MnSn MTJs, Fe(30 nm)/MgO(2.4 nm)/CoFe(10 nm) MTJs were also prepared. The magnetoresistance of the Fe/MgO/CoFe MTJs displayed large TMR ratio of about 170% at a bias voltage of +1 mV and the TMR ratio simply decreased with increasing the magnitude of bias voltage at 300 K. The sign change in the TMR ratio with changing temperature was not observed. These results mean that the anomalous TMR is a characteristic phenomenon for the Fe/MgO/Co₂MnSn MTJs.

IV. DISCUSSION AND A MODEL ANALYSIS

Let us start with discussion on the bias-voltage dependence of the TMR ratio. The bias-voltage dependence of the TMR ratio shown in Fig. 3(a) is asymmetric with respect to the positive and negative bias voltage. The asymmetry is due to an asymmetric structure of Fe/MgO/Co₂MnSn junctions. The tendency that the TMR ratio is positive (negative) in highly positive (negative) bias region is similar to that reported by Marukame *et al.*¹⁸ However, the magnitude of the TMR ratio is smaller near zero bias region in the present case as compared with their results. The negative TMR ratio in negative bias voltage region shown in Fig. 3(a) is caused by a reduction of RA in AP magnetization alignment as shown in Fig. 3(b). The reduction may be attributed to a characteristic change in the local densities of states (DOS) of Heusler alloy electrodes near the interface.^{23,26} The small TMR ratio near zero bias region might also be caused by a change in the local electronic states at the interface due to certain imperfections of the junction structure. Because the bandgap of Co₂MnSn at the Fermi level is narrow as compared with other Heusler alloys, which are expected as half metal materials, e.g., Co₂MnSi (Ref. 30), the spin polarization of Co₂MnSn might be decreased by slight defects.³¹

The sign change of the TMR ratio with changing temperature, on the other hand, has not been interpreted so far. Characteristic features of the temperature dependence of the TMR ratio can be seen in Figs. 3 and 4; the TMR ratios observed at three bias voltages change linearly with increasing temperature, the change in RA with temperature is larger in the AP alignment than in P alignment for all the three cases, and the sign change of the TMR ratio occurs at temperatures which is much lower than the Curie temperature. The observed features suggest that the sign change of the TMR ratio with temperature may not be attributed to any intrinsic origins such as spin fluctuations within magnetic electrodes, but to extrinsic origins such as structural and magnetic imperfections. We will attribute it to an extrinsic origin caused by a temperature dependent interaction of tunneling electrons with small spin-clusters within the insulating barrier. The tunneling electrons interact with the spin-clusters of the ground state at low temperature. With increasing temperature, they begin to interact also with the spin-clusters of the excited states, resulting in a sign change of the TMR ratio.

Before performing an analysis of the TMR ratio by using a concrete model system, we derive an expression of the TMR ratio which includes extrinsic spin-dependent effects caused within the insulating barrier. In the Jullière's model,³² the tunnel conductance Γ is proportional to products of DOS at the Fermi level $D_{L\sigma}(\varepsilon_F)$ and $D_{R\sigma'}(\varepsilon_F)$ of left (L) and right (R) electrodes, respectively, and spin-independent transmission probability T , where σ and σ' denote majority (+) and minority (−) spin states. Caroli *et al.*³³ have given an explicit expression of T , as $T \sim |tg t'|^2$ using the non-local Green's function g within the barrier and hopping integrals t (t') between the left (right) electrodes and the barrier. Because g is spin-dependent in general, the tunnel conductance may be given with spin-dependent transmission probability $T_{\sigma\sigma'}$ as

$$\Gamma \simeq \frac{2\pi e^2}{\hbar} \sum_{\sigma} D_{L\sigma}(\varepsilon_F) D_{R\sigma'}(\varepsilon_F) T_{\sigma\sigma'}, \quad (1)$$

where $\sigma' = \sigma$ for the conductance Γ_P in the P alignment and $\sigma' = -\sigma$ for the conductance Γ_{AP} in the AP alignment. The spin dependence of $T_{\sigma\sigma'}$ is governed by the spin dependence of the local Green's function g . A modified expression of the TMR ratio may be obtained by using a conventional definition of the spin polarization $P_{L(R)}$ of DOS of left (right) electrode,

$$D_{X+(-)}(\varepsilon_F) = D_{X0}(\varepsilon_F) [1 + (-)P_X], \quad (2)$$

with $X = L$ or R .

It should be noted that the decoupling of the conductance in terms of DOS and spin-dependent transmission probability may not be appropriate for coherent tunneling e.g., in Fe/MgO/Fe junctions. When spin-dependence of $T_{\sigma\sigma'}$ originates from a certain extrinsic origin, such as a spin-cluster within the tunnel barrier, it may depend solely on the spin of tunneling electrons, up (\uparrow) or down (\downarrow). Here we define \uparrow and \downarrow spins in the following way. As described before, the sample quality may be less perfect near the Co₂MnSn (L-electrode)/MgO interface than near the MgO/Fe (R-electrode) interface, such spin-clusters may reside near the Co₂MnSn/MgO interface and weakly couple with Co₂MnSn magnetization due to an effective magnetic field from Co₂MnSn. (See inset of Fig. 5.) The magnetic coupling of the spin-clusters and Co₂MnSn magnetization may be unchanged even when the Fe magnetization is reversed from P to AP alignment as done in experiments. We then assume that the \uparrow and \downarrow spins of tunneling electrons are governed by the spin axis in the Co₂MnSn electrode.

With this definition of up (\uparrow) and down (\downarrow) spins, we may assume that $T_{++} = T_{+-} = S_{\uparrow}$ and $T_{--} = T_{-+} = S_{\downarrow}$. The tunnel conductance in P(AP) alignment $\Gamma_{P(AP)}$ is then given as

$$\Gamma_{P(AP)} = \Gamma_0 [(1 + P_L)\{1 + (-)P_R\}S_{\uparrow} + (1 + P_L)\{1 - (+)P_R\}S_{\downarrow}], \quad (3)$$

where Γ_0 is a conductance in the non-magnetic state. The TMR ratio defined as $\text{TMR} = (\Gamma_P - \Gamma_{AP})/\Gamma_{AP}$ is given as,

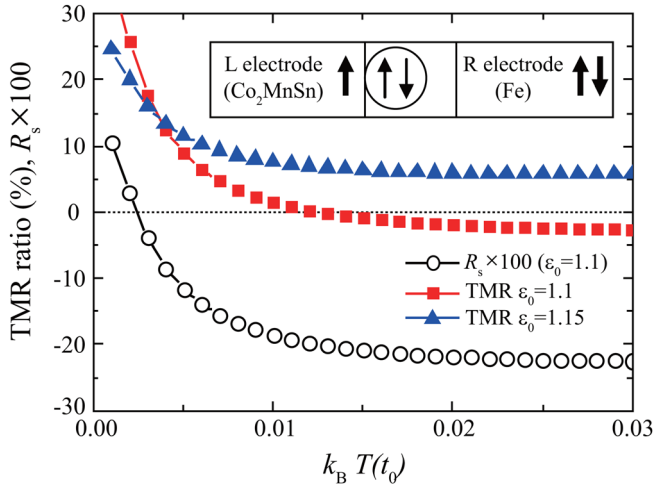


FIG. 5. (Color online) Calculated results of TMR ratios as a function of temperature for two values of impurity level ε_0 . Results of R_s with $\varepsilon_0 = 1.1$ are also presented. Parameter values are $J = 0.01$, $K = 0.01$, and $h = 0.018$. (See the Appendix for details.) Inset shows a schematic figure for the position of a spin-cluster in MTJs.

$$\text{TMR} = \frac{2P_R(P_L + R_s)}{1 - P_L P_R + (P_L - P_R)R_s}, \quad (4)$$

with

$$R_s = \frac{S_\uparrow - S_\downarrow}{S_\uparrow + S_\downarrow}, \quad (5)$$

where R_s represents the spin asymmetry of the tunneling probability. The Eq. (4) is a modified Jullière's TMR ratio. The TMR ratio can be negative when $P_L + R_s < 0$ even for junctions with $P_L, P_R > 0$. When S_σ changes with temperature, the sign of $P_L + R_s$ and of TMR ratio may reverse as a function of temperature.

Now we specify the model system for the interaction between a tunneling electron and a spin-cluster within the tunnel barrier (See the Appendix for more details). As the spin-cluster, we take into consideration of two localized spins with $S = 1/2$ coupled each other by a parameter $J(> 0)$, for simplicity. Electrons transport from L-electrode to R-electrode and interact with the localized spins within the insulator. The interaction is characterized by a parameter $K(> 0)$. Zeeman energy, which is produced by ferromagnetic electrodes on localized spins, is characterized by a parameter h .

By using the model, temperature dependence of the TMR ratio and R_s may be argued as follows. Eigenvalues of isolated localized spins within the insulator are $-3J, J$ and $J \pm h$. The first one is the eigenvalue of the singlet state, and the latter three are those of triplet states being split by the effective field. For argument below, let us use expressions that $(\uparrow\downarrow)$ state denotes the singlet one, and $(\uparrow\uparrow)$ and $(\downarrow\downarrow)$ states denote triplet ones with eigenvalues $J - h$ and $J + h$, respectively.

At low temperature, tunneling electrons interact with the ground state (singlet state) of the localized spins, because of $J > 0$. Since there is no net local moment in the singlet state, one might be inclined to think that there is no spin-dependence

in electron transmission through the insulator. We find it incorrect when we take into consideration the intermediate spin configurations caused by the interaction between tunneling electrons and localized spins. When an \uparrow spin electron interacts with the localized spins of the $(\uparrow\downarrow)$ state, a configuration with a \downarrow spin electron and $(\uparrow\uparrow)$ localized spins appears. On the other hand, when a \downarrow spin electron interacts with the localized spins of the $(\uparrow\downarrow)$ state, a configuration with \uparrow spin electron and $(\downarrow\downarrow)$ localized spins appears. Because the energy of the $(\uparrow\uparrow)$ state is lower than that of the $(\downarrow\downarrow)$ state due to the effective field, the \uparrow spin electrons are easier to transmit the insulator than the \downarrow spin electrons, that is, $S_\uparrow > S_\downarrow$.

At high temperature, tunneling electrons may interact directly with the excited spin states of the localized spins. When an \uparrow spin electron interacts with the first excited $(\uparrow\uparrow)$ state, no intermediate spin configuration appears due to the conservation of the total spins. When a \downarrow spin electron interacts with the localized spins of the $(\uparrow\uparrow)$ state, several intermediate spin configurations appear, which increases the number of tunneling path, and as a result the conductance increases. In addition, the interaction energy between a \downarrow spin electron and the localized spins of the $(\uparrow\uparrow)$ state is lower than that between an \uparrow spin electron and the localized spins of the $(\uparrow\uparrow)$ state, because $K > 0$. Therefore, \downarrow spin electrons become easier to transmit through the insulator than \uparrow spin electrons, and we get $S_\uparrow < S_\downarrow$. With raising temperature, the contribution of the $(\uparrow\uparrow)$ spin state increases gradually, and a sign change in R_s may appear.

There are two important ingredients in the argument above: one is a dynamical effect (transverse components) of the interaction between tunneling electrons and localized spins, and the other is a multisite interaction in localized spins. In order to incorporate these ingredients into the calculation of the tunnel conductance, we adopt so-called many body tight-binding method, which has been used to study a dynamics of a single hole in antiferromagnetic background,³⁴ and to calculate the conductance by using Kubo formula.³⁵ Here we apply it to the present system; a single tunneling electron and two localized spins. Details are presented in the Appendix.

Figure 5 shows calculated results of TMR ratios for two values of ε_0 , bare energy level of two sites in the insulator on which localized spins reside. Parameter values of K, J and h are $J = 0.01, K = 0.01$, and $h = 0.018$, respectively, in units of the hopping integral t_0 (~ 1 eV). These values are assumed by taking into consideration that the sign change in TMR ratios occurs around 10^2 K. Values of P_L and P_R are assumed to be 0.2 and 0.5, respectively, by considering following experimental results. The observed TMR ratio 170% for Fe/MgO/CoFe MTJs indicates that the effective spin polarization Fe (R-electrode) is about 0.7, while the TMR ratio in Fe/Al-O/Fe gives $P_{\text{Fe}} \sim 0.3 - 0.4$ (Refs. 1 and 2). Therefore, we take $P_R = 0.5$. The spin polarization of Co_2MnSn (L-electrode) could be rather small because the TMR ratios observed are small. We have observed around 20% TMR ratio for some MTJs with Co_2MnSn . In this case, using the Jullière's expression and $P_R = 0.5$, we obtain $P_L \sim 0.2$.

Calculated results in Fig. 5 show that the TMR ratios are enhanced at low temperatures and decrease with increasing temperature and change the sign in some cases. Results with open circles show the temperature dependence of R_s for $\varepsilon_0 = 1.1$. The sign change in the TMR ratios is caused by the sign change in R_s as explained before. When ε_0 is large, the effective energy levels of tunneling electrons are much higher than the Fermi energy, and the temperature dependence of the TMR ratio is weak, resulting in positive TMR ratios for all the temperatures. When ε_0 becomes small, there appears a sign change in the TMR ratio. We note that the sign change with changing temperature does not appear in the calculated results when the parameter P_L is large. This is why the sign change with changing temperature is not observed for MTJs using high spin polarized electrodes, e.g., Co_2MnSi .

Although our results can reproduce a sign change in the TMR ratio with increasing temperature at zero bias voltage, they are unable to reproduce the linear temperature dependence in Fig. 4. A simple model containing only two localized spins might be a possible reason. In the present choice of parameter values, the results do not produce a negative TMR ratio for all temperature range. However, when we assume that a parallel spin state of the triplet states is the ground state, \downarrow spin electrons are much easier to tunnel through the insulator, and the TMR ratio becomes negative for all the temperature range. Since the value of ε_0 may be changed by bias voltage, the temperature dependence of the TMR ratio is also dependent on bias voltage.

Thus, we suggest that the intermediate states caused by the dynamical interaction of tunneling electrons with localized spins is quite important for the temperature dependence of TMR ratios.

V. CONCLUSION

In this study, we performed the magnetoresistance measurements for the epitaxial $\text{Fe}/\text{MgO}/\text{Co}_2\text{MnSn}$ MTJs at various bias voltages and temperatures. The sign change of TMR effect was observed for the TMR measurement as a function of bias voltage. The sign change of TMR effect also occurred with changing bias voltage. A modified Jullière's model which adopts an interaction between a tunneling electron and localized spins of magnetic impurities in an insulator allows the generation of positive and negative TMR ratios. These results indicate that the reduction of electron scatterings within the insulator will be key to enhance the TMR ratios.

ACKNOWLEDGMENTS

The authors thank Dr. Y. Sakuraba of Tohoku University for fruitful discussion. This work was supported by Grant-in-Aid for Scientific Research in Priority Areas "Creation and Control of Spin Current" (Grant Nos. 21019008, 19048023, and 19048022) from the Ministry of Education, Culture, Sports, Science and Technology of Japan. This work was also supported by Collaborative Research Program of Institute for Chemical Research, Kyoto University (Grant No. #2010-43) and Institute of Ceramics Research and Education, Nagoya Institute of Technology.

APPENDIX: MODEL AND FORMALISM FOR TEMPERATURE DEPENDENCE OF TMR EFFECT

Figure 6 shows schematics of the MTJ. The quantity S_σ defined in section IV is evaluated for a one-dimensional lattice which is divided into three parts, left (L)-chain, right (R)-chain and an insulator. L-chain and R-chain correspond to the left and right electrode, respectively. We assume that two localized spins exist within the insulator and interact with tunneling electrons. The Hamiltonian of the junction is given as,

$$H = H_L + H_R + H_t + H_c, \quad (\text{A1})$$

where H_L and H_R are the Hamiltonian of L- and R-chains, respectively, which are characterized by a hopping integral t_0 , and

$$H_t = \sum_{\sigma} (tc_{m\sigma}^\dagger c_{1\sigma} + t'c_{2\sigma}^\dagger c_{n\sigma} + hc), \quad (\text{A2})$$

$$H_c = \sum_{i\sigma} \varepsilon_{i\sigma} c_{i\sigma}^\dagger c_{i\sigma} - \tau \sum_{\sigma} (c_{1\sigma}^\dagger c_{2\sigma} + c_{2\sigma}^\dagger c_{1\sigma}) + \sum_{i=1,2} K S_i \cdot \sigma_i + J S_1 \cdot S_2 - \sum_{i=1,2} h_i S_{iz}. \quad (\text{A3})$$

Here, H_t represents hopping of electrons between L(R)-chain and site 1(2) within the insulator. H_c denotes the Hamiltonian for electrons and spins in the insulator; $\varepsilon_{i\sigma}$ the energy level on site $i (= 1, 2)$, τ a hopping integral between sites 1 and 2, K the interaction between localized spins S and tunneling electron with spins σ , and J the interaction between localized spins. The last term is a Zeeman term in which h_i is an effective magnetic field acting on spins on the i -th site. We assume that the effective field is produced by ferromagnetic electrodes. We take into account both transverse and longitudinal components of the interactions, which are characterized by parameters K_\perp , K_\parallel , J_\perp , and J_\parallel . In the following, we assume that both S and σ are expressed by Pauli matrices.

We formulate the tunnel conductance for parallel (P) and antiparallel (AP) alignments of magnetizations on left and right electrodes, assuming incoherent tunneling and preparing basis functions which include states of both tunneling electron and localized spins. In the present mode, we have 16 basis functions given as $|n\sigma\mu\rangle = |n\sigma\rangle \otimes |\mu\rangle$, where $n = 1, 2$, $\sigma = \uparrow, \downarrow$ and $|\mu\rangle$ indicates singlet and triplet states of two localized spins. This kind of formulation is called configuration interaction method or many-body tight-binding (TB)

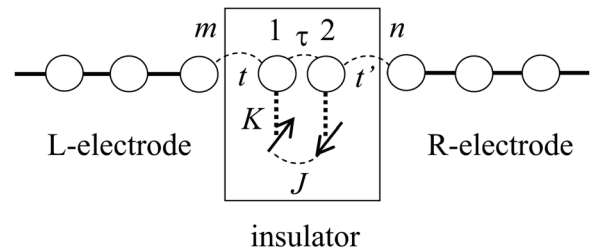


FIG. 6. Model used to calculate the conductance of the junction which includes two magnetic impurities within the insulator.

method.^{34,35} Using these basis states, we prepare a variational function $\psi = n_{\sigma\mu} a_{n\sigma\mu} |n\sigma\mu\rangle$, and express matrix element of the Green's function g_{12} analytically.

The meaning of the term $|tg_{12}t'|^2_\sigma$ that is defined as S_σ is explained in a following way. An electron with spin σ enters to site 1 in the insulator from L electrode and hops to site 2 and goes out to R electrode. This is the process given by $tg_{12}t'$. A reversed process is given by $(tg_{12}t')^\dagger$. In these processes the electron interacts with two localized spins. Since there are many spin configurations, several hopping processes occur. Examples of hopping processes are given in Fig. 7, where Fig. 7(a) shows a representation of the many-body states, Fig. 7(b) shows a process in which tunneling electron has \downarrow spin and the localized spins are parallel, and Fig. 7(c) shows a process in which the tunneling electron has \uparrow spin. We see that the former process has many intermediate states.

Now we have two remarks. First, the tunneling process of $|tg_{12}t'|^2$ is such a process that starts from the initial state and ends at the final states via intermediate states of localized spins. Therefore, the initial and final states should be identical. Secondly, the tunneling electron does not interact with all spin configurations in equal weight. Because the weight may depend on temperature, we introduce a Boltzmann factor,

$$S_\sigma = \sum_\mu S_{\sigma\mu} e^{-(E_\mu - E_G)/k_B T}, \quad (\text{A4})$$

where μ stands for the eigenstate of two localized spins, $S_{\sigma\mu}$ is a matrix element of $|tg_{12}t'|^2_\sigma$ with μ -th spin configuration, E_G the ground (singlet) state energy, and k_B is the Boltzmann constant.

Numerical results shown in Fig. 5 are calculated by assuming that $\varepsilon_{1\uparrow} = \varepsilon_{1\downarrow} = \varepsilon_{2\uparrow} = \varepsilon_{2\downarrow} \equiv \varepsilon_0$, $J_{\parallel} = J_{\perp} \equiv J = 0.01$, $K_{\parallel} = K_{\perp} \equiv K = 0.01$, and $h_1 = h_2 = h = 0.018$, for $\varepsilon_0 = 1.1 - 1.15$ in units of t_0 . Values of P_L and P_R are 0.2 and 0.5, respectively. Because t_0 of metals or transition metal oxides is of order 1 eV, so a value of energy 0.01 corre-

sponds 100 K. The values are chosen from the following reasons. When the localized spins are produced by excess electrons or holes around defects in a MgO layer, the interaction J may be 0.001 eV (Ref. 36). On the other hand, when they are produced by magnetic impurities, e.g., Co or Mn mixed into the MgO layer, the value of J may be larger than that between localized spins of excess electrons or holes around defects, and of an order of the Curie or Néel temperature, that is $J \sim 0.01$ eV. Therefore, the parameter value $J = 0.01$ is reasonable. The details of the tunnel barrier are included effectively in the parameters t, t', τ .

Because of the dynamical interaction of tunneling electrons with localized spins, R_s or S_σ are strongly temperature dependent, and TMR ratio may change the sign with temperature. In the present choice of parameter values, the ground state is the singlet and the triplet states are excited ones. Therefore, the tunneling electron interacts with the singlet state at low temperature. With increasing temperature, the second lowest energy state begins to contribute the tunneling, which is a triplet with parallel spins in the present case. Then the number of tunneling channel of \downarrow spin electrons increases as shown in Fig. 7(b). Increase of S_{\downarrow} gives rise to a negative value of R_s . It is noted that S_σ is dependent on the spin even when the tunneling electron interacts with the singlet state, because intermediate states caused by the interaction are not symmetrical with respect to the spin.

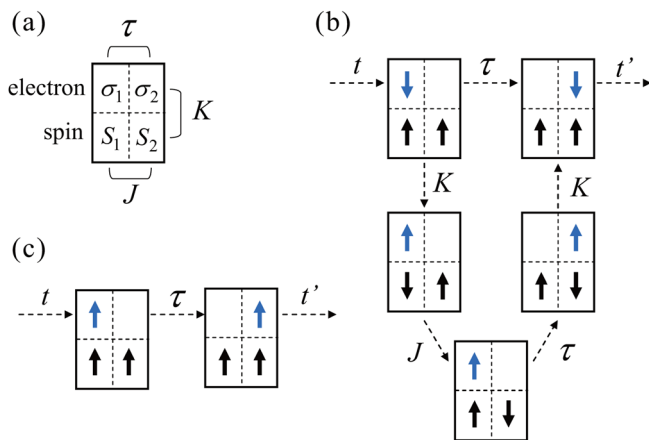


FIG. 7. (Color online) Example of tunneling process of an electron interacting with localized spins. (a) Representation of the many-body states, (b) tunneling process when a down spin electron enters the insulator and interacts with localized spins, and (c) tunneling process when an up-spin electron enters the insulator.

- ¹T. Miyazaki and N. Tezuka, *J. Magn. Magn. Mater.* **139**, L231 (1995).
- ²J. S. Moodera, L. R. Kinder, T. M. Wong, and R. Meservey, *Phys. Rev. Lett.* **74**, 3273 (1995).
- ³W. H. Butler, X.-G. Zhang, T. C. Schulthess, and J. M. MacLaren, *Phys. Rev. B* **63**, 054416 (2001).
- ⁴J. Mathon and A. Umerski, *Phys. Rev. B* **63**, 220403 (2001).
- ⁵S. Yuasa, T. Nagahama, A. Fukushima, Y. Suzuki, and K. Ando, *Nature Mater.* **3**, 868 (2004).
- ⁶S. S. P. Parkin, C. Kaiser, A. Panchula, P. M. Rice, B. Hughes, M. Samant, and S.-H. Yang, *Nature Mater.* **3**, 862 (2004).
- ⁷H. Itoh, *J. Phys. D: Appl. Phys.* **40**, 1228 (2007).
- ⁸Y. M. Lee, J. Hayakawa, S. Ikeda, F. Matsukura, and H. Ohno, *Appl. Phys. Lett.* **90**, 212507 (2007).
- ⁹S. Zhang, P. M. Levy, A. C. Marley, and S. S. P. Parkin, *Phys. Rev. Lett.* **79**, 3744 (1997).
- ¹⁰V. Drewello, J. Schmalhorst, A. Thomas, and G. Reiss, *Phys. Rev. B* **77**, 014440 (2008).
- ¹¹T. Obata, T. Manako, Y. Shimakawa, and Y. Kubo, *Appl. Phys. Lett.* **74**, 290 (1999).
- ¹²M. Bowen, M. Bibes, A. Barthélemy, J.-P. Contour, A. Anane, Y. Lemaître, and A. Fert, *Appl. Phys. Lett.* **82**, 233 (2003).
- ¹³V. Garcia, M. Bibes, A. Barthélemy, M. Bowen, E. Jacquet, J.-P. Contour, and A. Fert, *Phys. Rev. B* **69**, 052403 (2004).
- ¹⁴H. Itoh, T. Ohsawa, and J. Inoue, *Phys. Rev. Lett.* **84**, 2501 (2000).
- ¹⁵I. Takada, J. Ozeki, H. Itoh, and J. Inoue, *Phys. Status Solidi B* **244**, 4452 (2007).
- ¹⁶Y. Sakuraba, M. Hattori, M. Oogane, Y. Ando, H. Kato, A. Sakuma, T. Miyazaki, and H. Kubota, *Appl. Phys. Lett.* **88**, 192508 (2006).
- ¹⁷T. Ishikawa, T. Marukame, H. Kijima, K.-I. Matsuda, T. Uemura, M. Arita, and M. Yamamoto, *Appl. Phys. Lett.* **89**, 192505 (2006).
- ¹⁸T. Marukame, T. Ishikawa, K.-I. Matsuda, T. Uemura, and M. Yamamoto, *J. Appl. Phys.* **99**, 08A904 (2006).
- ¹⁹T. Taira, T. Ishikawa, N. Itabashi, K.-I. Matsuda, T. Uemura, and M. Yamamoto, *J. Phys. D: Appl. Phys.* **42**, 084015 (2009).
- ²⁰M. Leifzaić, Ph. Movropoulos, J. Enkovaara, G. Bihlmayer, S. Brügel, *Phys. Rev. Lett.* **97**, 026404 (2006).
- ²¹L. Chioncel, Y. Sakuraba, E. Arrigoni, M. I. Katsnelson, M. Oogane, Y. Ando, T. Miyazaki, E. Burzo, and A. I. Lichtenstein, *Phys. Rev. Lett.* **100**, 086402 (2008).

- ²²I. Galanakis, *J. Phys.: Condens. Matter*, **14**, 6329 (2002).
- ²³S. Picozzi, A. Continenza, and A. J. Freeman, *Phys. Rev. B* **69**, 094423 (2004).
- ²⁴M. Sharma, S. X. Wang, and J. H. Nickel, *Phys. Rev. Lett.* **82**, 616 (1999).
- ²⁵C. Heiliger, P. Zahn, B. Yu. Yavorsky, and I. Mertig, *Phys. Rev. B* **72**, 180406 (2005).
- ²⁶Y. Miura, K. Abe, and M. Shirai, *J. Phys.: Conf. Ser.* **200**, 052016 (2010).
- ²⁷C. Barraud, P. Seneor, R. Mattana, S. Fusil, K. Bouzehouane, C. Deranlot, P. Graziosi, L. Hueso, I. Bergenti, V. Dediu, F. Petroff, and A. Fert, *Nature Phys.* **6**, 615 (2010).
- ²⁸K. Mibu, D. Gondo, T. Hori, Y. Ishikawa, and M. A. Tanaka, *J. Phys.: Conf. Ser.* **217**, 012094 (2010).
- ²⁹M. A. Tanaka, T. Hori, S. Hori, K. Kondou, S. Kasai, T. Ono, and K. Mibu, *J. Phys.: Conf. Ser.* **266**, 012107 (2011).
- ³⁰Y. Kurtulus, R. Dronskowski, G. D. Samolyuk, and V. P. Antropov, *Phys. Rev. B* **71**, 014425 (2005).
- ³¹Y. Sakuraba, private communication (2011).
- ³²M. Jullière, *Phys. Lett. A* **54**, 225 (1975).
- ³³C. Caroli, R. Combescot, P. Nozieres, and D. Saint-James, *J. Phys. C: Solid State Phys.* **5**, 21 (1972).
- ³⁴J. Inoue and S. Maekawa, *J. Phys. Soc. Jpn.* **59**, 2110 (1990).
- ³⁵J. Inoue, N. Nishimura, and H. Itoh, *Phys. Rev. B* **65**, 104433 (2002).
- ³⁶A. M. Stoneham, A. P. Pathak, and R. H. Bartram, *J. Phys. C: Solid State Phys.* **9**, 73 (1976).